European Journal of Pharmaceutics and Biopharmaceutics 83 (2013) 168–173

Contents lists available at SciVerse ScienceDirect

European Journal of Pharmaceutics and Biopharmaceutics

journal homepage: www.elsevier.com/locate/ejpb

Research paper

Production of nanoparticles-in-microparticles by a double emulsion method: A comprehensive study

Yan-Sim Lee [a,*], Philip J. Johnson [b], Philip T. Robbins [a], Rachel H. Bridson [a]

[a] School of Chemical Engineering, University of Birmingham, Edgbaston, Birmingham, B15 2TT, UK
[b] School of Cancer Studies, University of Birmingham, Edgbaston, Birmingham, B15 2TT, UK

ARTICLE INFO

Article history:
Received 7 February 2012
Accepted in revised form 4 October 2012
Available online 12 November 2012

Keywords:
Nanoparticles-in-microparticles
Solid-in-water-in-oil-water emulsion
Drug delivery
PLGA
PCL
Solvent evaporation

ABSTRACT

A method based on a double emulsion system (solid-in-water-in-oil-in-water) has been developed for the production of nanoparticles-in-microparticles (NIMs). The distribution of nanoparticles within the NIMs was explored using light and electron microscopy and through assessment of drug loading and release profiles. The extent of nanoparticle entrapment within the NIMs was found to be dependent on the state (wet vs. dry) in which the nanoparticles were introduced to the formulation. The technique was readily adaptable to produce NIMs of different morphologies. It is proposed that NIMs and this method to produce them have broad application in drug delivery research.

1. Introduction

The applications of microparticles and nanoparticles as delivery vehicles or therapeutic entities are widely described in the literature. Their combination, for example, as nanoparticle-in-microparticle (NIM) systems, offers the possibility of dual or multiple functionalities within a formulation. For example, multiple release profiles (burst release from outer particles and sustained release from internal components) and/or combinations of features allowing site specificity, *in vivo* protection, cellular interactions, imaging capabilities and embolisation can all be envisaged. In recent examples, Veiseh et al. proposed multifunctional delivery systems comprising both imaging and therapeutic agents, in addition to a functionalised surface to enhance specific cell interactions [1]. Pouponneau et al. produced a microparticle system that encapsulated magnetic nanoparticles and showed that under the influence of a magnetic field, the particles could be steered *in vitro* [2]. Another example includes theophylline-loaded NIM suitable for asthmatic treatment in which Jelvehgari et al. utilised the outer microparticle as a means to reduce burst release [3].

Various methods have been proposed for the preparation of NIM systems. Spray drying techniques have been used to produce NIMs for aerosols [4–7], oral [8,9] and intravitreal formulations [10]. Other methods include supercritical fluid techniques [11–13]. There is, however, little information on how NIMs can be produced using the standard emulsion techniques that are widely and conveniently used in the preparation of particles for drug delivery research. Such methods for preparing single-component particles (i.e. microparticles or nanoparticles alone) are renowned for their application to both hydrophilic or hydrophobic drugs and a variety of polymer systems [14]. Additionally, through modification of process parameters, characteristics such as particle size distribution and morphology can be readily altered. While work such as Jelvehgari et al. [3] provides methodology for NIM formation, there is little convincing information in the drug delivery literature on the internal structure of NIMs or the distribution of nanoparticles therein. Given that this could have profound effects on characteristics such as release profiles or *in vivo* distribution (e.g. whether nanoparticles remain internalised or readily 'escape') it is important to understand the relationship between the production technique and the structure of the resulting product.

The aim of the work described in this paper was to explore the production of NIMs using a method based on traditional 'double emulsion' techniques that are conventionally employed to make drug-loaded microparticles. The distribution of nanoparticles within the resulting NIM formulations was investigated, drawing on evidence from imaging of the emulsion systems and the final particle products and also through characterisation of drug loading/release profiles. As stated earlier, NIMs have the broad range of potential pharmaceutical uses. In this work, we had the application of chemoembolisation in mind, where the inner nanoparticles are

* Corresponding author. School of Chemical Engineering, Bldg. Y11, Room 117, University of Birmingham, Edgbaston B15 2TT, UK. Tel.: +44 (0) 121 414 5081; fax: +44 (0) 0121 414 5377.
E-mail address: ian.yansimlee@gmail.com (Y.-S. Lee).

0939-6411/$ - see front matter © 2012 Elsevier B.V. All rights reserved.
http://dx.doi.org/10.1016/j.ejpb.2012.10.016

drug delivery vehicles and the outer microparticles act as embolisation agents for cutting off the blood supply to tumours.

2. Materials and methods

2.1. Materials

Poly(ε-caprolactone) (PCL), hydrocortisone acetate (HA), poly(vinyl alcohol) (PVA), SPAN 80 and Nile red were purchased from Sigma–Aldrich, UK. 50:50 poly(lactic-co-glycolic) acid (PLGA), isomeric poly(L-lactic acid) (PLLA) and poly(DL-lactic acid) (PDLA) were purchased from SurModic Pharmaceutical Inc., USA. Dichloromethane (DCM), ethyl acetate (EA), acetonitrile (MeCN), acetone, fluorescein, sodium acetate (NaOAc), sodium chloride, citric acid, sodium hydroxide and acetic acid glacial were purchased from Fisher Scientific, UK.

2.2. Production of drug-loaded nanoparticles

PCL nanoparticles loaded with HA were prepared for the study as follows: A solution of PCL in acetone (1% w/w) was prepared to which HA was added, producing a drug-to-polymer mass ratio of 1:2. 5 mL of the drug/polymer solution was then emulsified in 200 mL of 1% w/w PVA solution. The stirring was continued for 4 h for the particles to solidify. After that, the particles were collected by centrifugation, and the supernatant decanted off. Before the resultant nanoparticles (N) were further used in the production of NIMs, they were either resuspended in 1 mL of 1% PVA solution to produce a slurry of wet nanoparticles (N_{slurry}), or oven-dried at 40 °C to produce dry nanoparticles (N_{dried}). For visualisation studies, Nile red was used in the place of HA.

2.3. Production of NIMs

Two formulations were produced; NIMs formulated either with the oven-dried nanoparticles (NIM_{dried}) or with the wet slurry nanoparticles (NIM_{slurry}). For the NIM_{dried} formulation, 40 mg of N_{dried} was homogenised in 0.5 mL of 1% w/w PVA solution ($[w_1]$), and then homogenised (IKA Ultra-Turrax® T25 Digital homogeniser, Janke & Kunkel GMBH & Co. KG., Germany) in 3 mL of 1% w/w 50:50 PLGA solution dissolved in EA (i.e. [o]) with 0.02 g of SPAN 80. The $[N_{dried}/w_1/o]$ primary emulsion was then added dropwise to 200 mL of 0.5% w/w PVA solution (i.e. $[w_2]$) under continuous magnetic stirring to form the double emulsion. The stirring was continued for 4 h for solvent evaporation and polymer solidification. Product recovery was by filtration and washing with 600 mL of distilled water. They were then oven-dried at 37 °C and stored in a dessicator until further analysis. For the NIM_{slurry} formulation, 0.5 mL of the N_{slurry} was used instead of N_{dried}. HA-loaded microparticles were prepared for comparison with the NIMs. These were prepared using a similar method to that used for the NIMs; however, in the absence of nanoparticles 0.015 g of HA was added directly to the 3 mL [o] phase of 1% w/w PLGA solution. Their average size was 113 ± 10 μm, with drug loading (see Section 2.4) of 3.43 ± 0.73%. Further studies to investigate how particle morphology and size could be manipulated were carried out with PLLA and PDLA (dissolved in DCM). The PLA's solutions were incorporated into the [o] phase with PLGA at a PLGA/PLA volume ratio of 1/2, all polymer solution at 1% w/w.

2.4. Drug loading and in vitro release studies

Drug quantification was achieved using HPLC (Shimadzu HPLC system equipped with a SCL-10A system controller, LC-10AD pump, SIL-10AD auto injector, CTO-10A column oven and SPD-10AV UV detector units) with a Sunfire™ column (C18 3.5 μm, 4.6 × 100 mm with a guard cartridge (4.6 × 20 mm) (Waters, UK). The chromatographic conditions were injection volume = 50 μL, flow rate = 1.0 mL min^{-1}, mobile phase = 30/70 MeCN/NaOAc buffer (pH 2.65), and UV detection at λ = 248 nm. To determine drug loading, approximately 8–10 mg of drug-loaded particles was dissolved in 50 mL of MeCN. Prior to injection, 1 volume of the sample solution was mixed with 2 volumes of the mobile phase. Drug loading was defined as below:

$$\%\ \text{drug loading} = [\text{amount of drug/total dry particle mass}] \times 100\% \quad (1)$$

In vitro drug release studies were carried out in a USP Type II dissolution apparatus. Approximately 8–10 mg of drug-loaded particles was incubated in 1 L of citric acid buffer (pH 4, in which drug sink conditions could be readily maintained) at 37 °C and 150 rpm. Solution sampling was carried out at regular intervals. A 2 mL aliquot was collected at each sampling point and replaced with an equal volume of fresh buffer. Drug concentration was determined using HPLC (as above).

2.5. Particle characterisation

The particle size distributions of NIMs were measured using laser diffraction particle sizing (Mastersizer 2000, Malvern Instruments, UK) giving overall average from three independent formulations each measured at least three times (± standard error of the mean). Size analysis using photon correlation spectroscopy (High Performance Particle Sizer, Malvern Instruments, UK) showed the nanoparticles to be 513 ± 46 nm in *z*-average diameter. Fluorescent microscopy was carried out using an Axiolab (Carl Zeiss Ltd.) fluorescence microscope. Confocal imaging was done using a Carl Zeiss LSM 510 microscope equipped with an argon photon laser (laser power, 10–75%) with excitation wavelength, λ = 488 nm and LP 505 filter. Image viewing and processing were performed using LSM 510 software.

The morphology of particles was assessed using a Philips XL30 scanning electron microscope. Prior to imaging, the specimens were mounted on a stub and platinum coated for 3 min using an EMscope SC 500 sputter coater (Quorum Technologies, UK). Cryo-fracture SEM to reveal the internal structure of NIMs was performed using a Philips XL30 Environmental Scanning Electron Microscopy with Field Emission Gun. For specimen preparation, a suspension of the microparticles in distilled water was placed into a four well stub specimen holder that then underwent rapid freezing in liquid nitrogen. The holder was then inserted into the cryo-preparation chamber attached to the SEM unit, which was maintained under vacuum at 10^{-5} Torr and −180 °C. Specimen fracturing was achieved *in situ* with a razor slicing through the frozen specimen. The fractured specimen was then gold-coated *in situ* for 3 min before being transferred into the imaging chamber for imaging at a typical acceleration voltage of 3 kV.

3. Results and discussion

3.1. Distribution of nanoparticles within the primary $[w_1/o]$ emulsion

The first stage in the production of NIMs is to prepare a stable primary emulsion $[w_1/o]$. With further processing steps (Section 2.3), the aqueous phase $[w_1]$ becomes the interior of the particle and the organic phase [o], the particle wall. The distribution of nanoparticles within the primary emulsion therefore influences their ultimate destination in the final NIMs. Fig. 1A and B illustrates how the N_{slurry} had a tendency to accumulate in $[w_1]$, which, as discussed below, appears to have facilitated to their subsequent

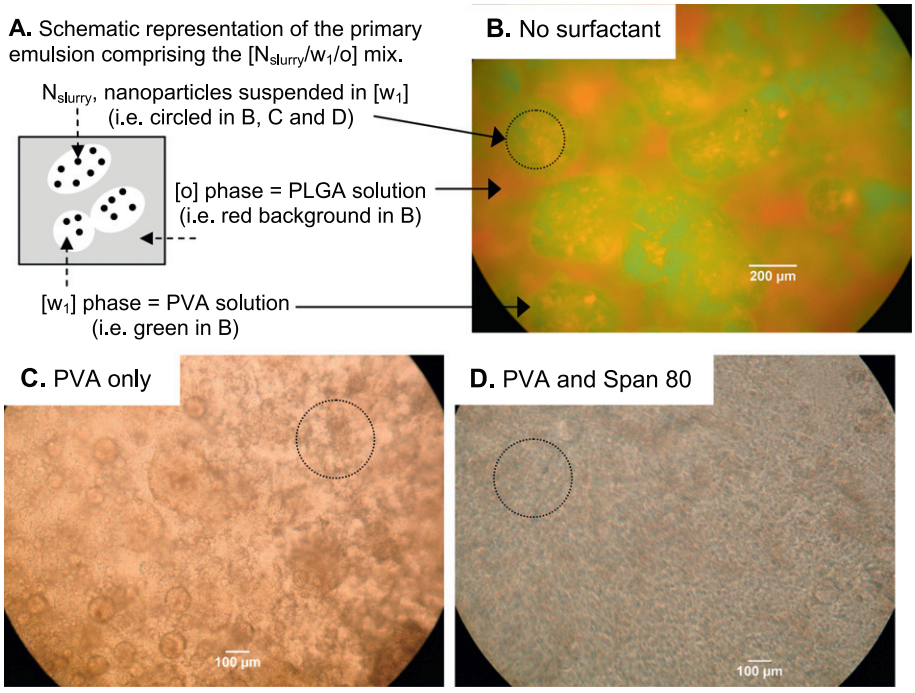

Fig. 1. (A) A schematic illustration of the primary emulsion comprising the [$N_{slurry}/w_1/o$] mix. (B) Fluorescent microscopy images showing the suspension of slurry nanoparticles (N_{slurry}) in the primary emulsion with no emulsifier. Fluorescein and Nile red were used to stain the PVA [w_1] phase and PLGA [o] phase, respectively. (C) Only PVA and (D) both PVA and SPAN 80 were used in the primary emulsion. (For interpretation of the references to colour in this figure legend, the reader is referred to the web version of this article.)

internalisation within the microparticles. In addition to ensuring such residency of the nanoparticles in the correct phase of the emulsion, it is also important to ensure proper emulsification of the immiscible [w_1] and [o] phases, so that nanoparticles are distributed throughout the microparticle population. In Fig. 1C and D, the importance of the two emulsifiers, PVA and SPAN 80, used in the primary emulsion can be seen. While PVA will adsorb at phase interfaces and stabilize emulsions via a steric hindrance effect [15], the SPAN 80, with a hydrophile-lipophile balance of 4.3, is important in the formation of the initial water-in-oil emulsion system [16].

3.2. Distribution of nanoparticles within NIM formulations: NIM_{slurry} vs. NIM_{dried}

With reference to Figs. 2 and 3, comparisons between the nanoparticle distribution of NIM_{dried} and NIM_{slurry} can be made, the former being associated with lower nanoparticulate encapsulation. Indeed for NIM_{dried}, a non-entrapped agglomerated mass of nanoparticles was evident around the exterior of the microparticles when examined under the light microscope (Fig. 2B) and nanoparticles were also seen on the outer surface of microparticles under the SEM (Fig. 3A). While it is difficult to determine from the confocal microscopy images shown in Fig. 3C and D whether the nanoparticles are within the wall of the microparticles or surface associated, the intensity of the nanoparticle signal is much stronger in Fig. 3D than for Fig. 3C, indicating better entrapment or improved nanoparticle loading with NIM_{slurry}.

PCL nanoparticles are known to be hydrophobic [17], which will naturally hinder their suspension in the internal aqueous phase [w_1]. Given the improved nanoparticle entrapment seen with NIM_{slurry} (Figs. 2C, 3B and D), it appears that the maintenance of the wet state/absence of the oven-drying stage in the preparation of N_{slurry} was important. This helped to impart surface characteristics that facilitated nanoparticle residency in [w_1] and/or prevented drying-induced augmentation of the hydrophobicity associated with PCL. With respect to the former hypothesis, maintaining the wet state of the nanoparticles and resuspending them immediately in PVA solution may have allowed a satisfactory PVA 'corona' to form around the nanoparticles. It has previously

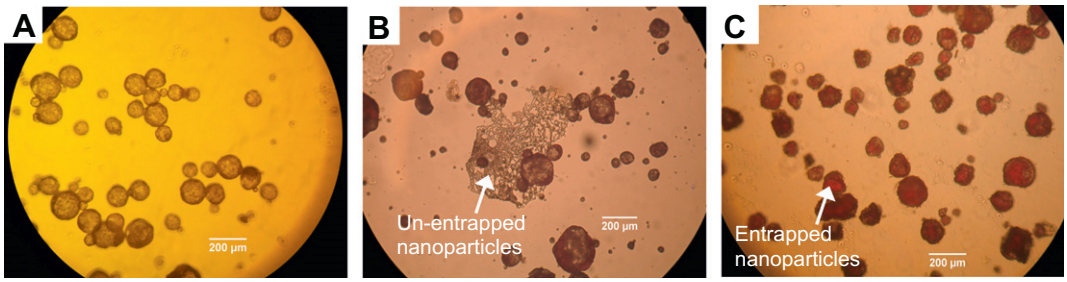

Fig. 2. Images obtained using a fluorescent microscope showing: (A) blank PLGA microparticles (no nanoparticles), (B) NIM_{dried} and (C) NIM_{slurry} where the Nile red stained nanoparticles can be seen. (For interpretation of the references to colour in this figure legend, the reader is referred to the web version of this article.)

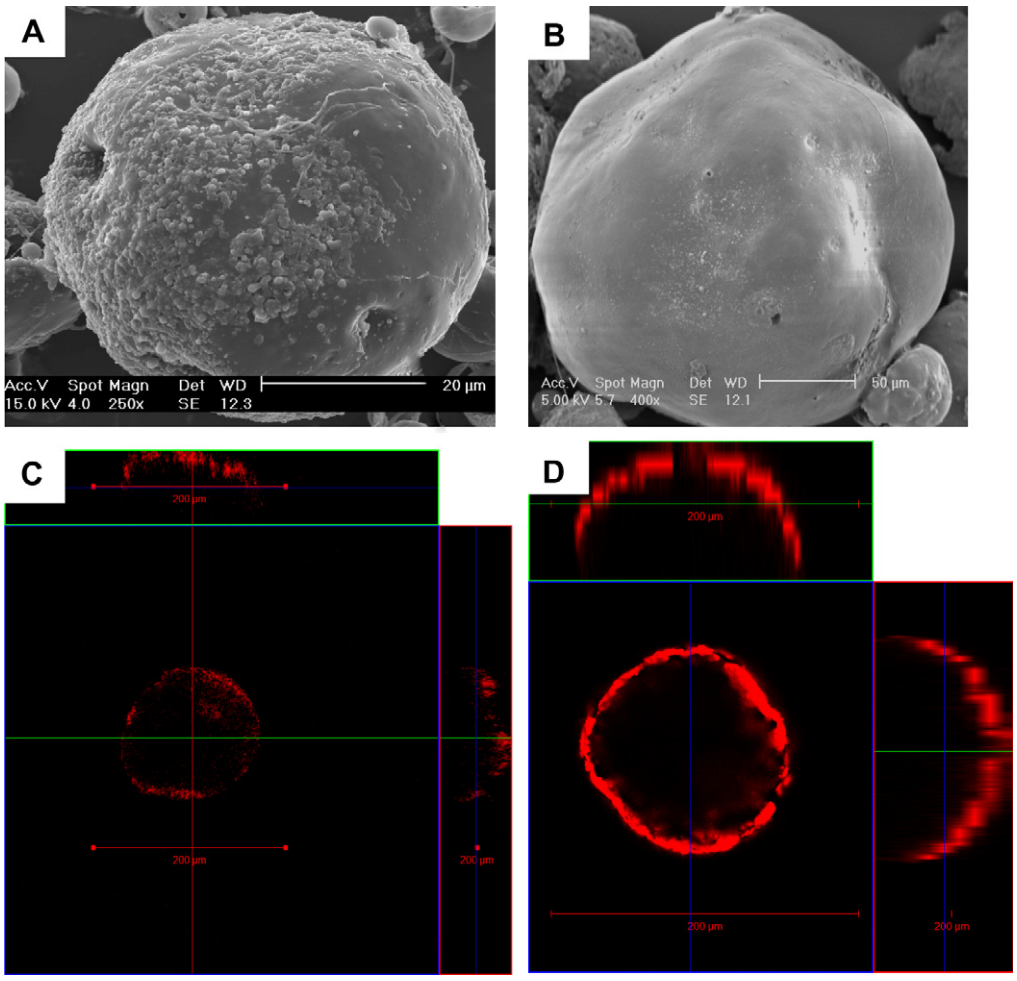

Fig. 3. A comparison of NIM_{dried} and NIM_{slurry} particles prepared using dry and wet nanoparticles in the primary emulsions, respectively. SEM images of (A) NIM_{dried} and (B) NIM_{slurry}. Confocal images of (C) NIM_{dried} and (D) NIM_{slurry}. (For interpretation of the references to colour in this figure legend, the reader is referred to the web version of this article.)

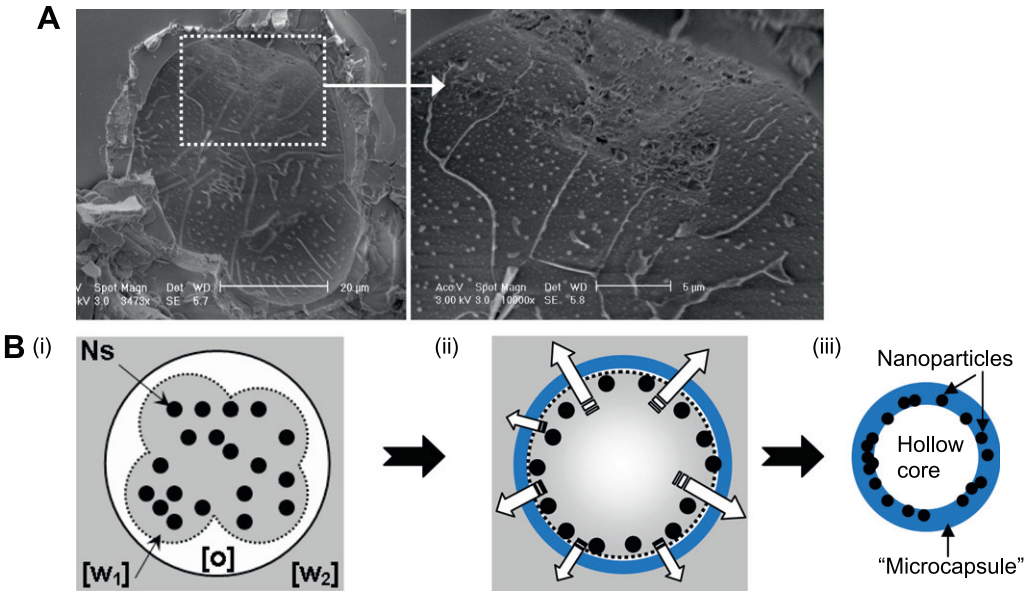

Fig. 4. (A) Cryo-fracture SEM images showing a cross sectional view of a NIM_{slurry} particle, revealing entrapped nanoparticles. (B) Suggested mechanism for how nanoparticles become wall-associated: (i) The $[N_s/w_1/o/w_2]$ emulsion system is created upon mixing of the four components; (ii) a "polymeric shell" is instantaneously formed due to rapid solvent diffusion and polymer solidification. The aqueous phase continues to diffuse out, transporting dissolved solvent through the shell and the nanoparticles (which are suspended in w_1) to the shell wall, where they are too large to pass through; (iii) the nanoparticles are trapped at the shell wall and a hollow core is seen. Ns = nanoparticles suspended in PVA solution or slurry nanoparticles. (For interpretation of the references to colour in this figure legend, the reader is referred to the web version of this article.)

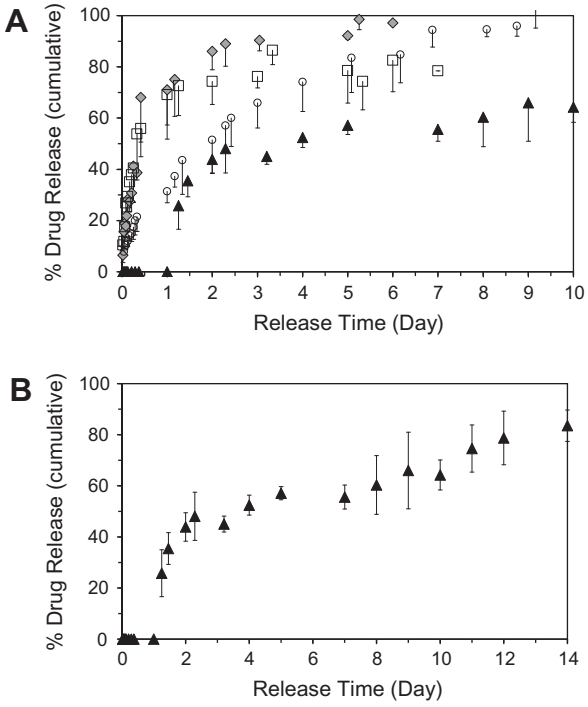

Fig. 5. (A) *In vitro* drug release profiles of HA-loaded PCL nanoparticles (◈), HA-loaded PLGA microparticles (○), NIM_{dried} (□) and NIM_{slurry} (▲) for all four systems. (B) Drug release over a period of 2 weeks for NIM_{slurry}. Results = mean ± standard deviation, $n = 3$ independent formulations.

been suggested that PVA can strongly absorb on the surface of protein-loaded PLGA nanoparticles [18], while its hydroxyl groups have also been envisaged to fix to the acetyl group of PLGA and thus improving the rehydration-ability of freeze-dried nanoparticles [19]. In the present work, the vinyl acetate segment of the partially hydrolysed PVA could have interpenetrated with the PCL molecule when the solvent diffuses towards the aqueous phase during the polymer solidification process [20]. The adsorption of PVA on polymeric particles surface during their preparations is common [21–23]. It could be suggested that subsequent drying has disrupted the interaction between the PVA and the PCL molecules resulting in a more hydrophobic product (i.e. N_{dried}).

Fig. 4A shows that when fractured to reveal their interiors, NIM_{slurry} particles are seen to have a hollow core with nanoparticles embedded within the wall of the microparticles. A mechanism leading to nanoparticle residency in the wall is proposed in Fig. 4B. The hollow core may be advantageous if capacity for the encapsulation of other agents is desired. Alternatively, if disadvantageous (e.g. leading to mechanical weakness), decreasing the volume of $[w_1]$ or reducing water droplet size could be employed to reduce the volume of the void, or redistribute it into a number of smaller, individual voids.

3.3. Drug loading and release profiles

To determine the drug loading of typical NIM systems, three separate batches of NIM_{dried} and NIM_{slurry} were prepared and three samples taken from each for analysis. Drug loadings were found to be 3.80 ± 0.82% and 6.46 ± 1.26% for NIM_{dried} and NIM_{slurry}, respectively. This difference is statistically significant (Mann–Whitney *U*-Test; $\alpha = 0.05$), again suggesting improved nanoparticle entrapment for NIM_{slurry}. The *in vitro* cumulative drug release profiles are shown in Fig. 5 and provide further evidence of the different entrapment profiles for NIM_{slurry} and NIM_{dried}. For the latter, the drug release profile was very similar to that seen for nanoparticles alone, supporting other evidence that the nanoparticles were largely surface associated (Fig. 3A). For NIM_{slurry}, an initial lag phase was observed (no release for ~1 day; only 'noise' on HPLC chromatograms). This may be due to the time required by the polymer of the outer microparticle to become hydrated [24] and provides clear evidence of nanoparticle internalisation. When the polymer becomes hydrated, its glass transition temperature is lowered and it will undergo phase transition from a glassy state to a rubbery state. The mass transfer resistance is thus lowered, and this permits subsequent solute transport and drug diffusion from the entrapped nanoparticles.

3.4. Control of NIM size and morphology

Fig. 6A shows that the NIMs prepared from PLGA (as described in Section 2.3) tended to be of irregular and non-spherical morphology. By introducing PDLA and PLLA into the [o] phase with PLGA at the ratio of PLA-to-PLGA of 1:2, the morphology could be manipulated (Fig. 6B and C). The change in polymer and corresponding change in viscosity was also hypothesised to provide a means for controlling the size of the NIMs. The PLGA systems, NIM_{dried} and NIM_{slurry}, were found to have average sizes of 145 ± 19 μm and 132 ± 24 μm, respectively (from laser diffraction particle sizing, three independent formulations, mean ± standard deviation). With equivalent homogenisation conditions during formulation (i.e. same energy input into the system), this increased to 405 ± 54 μm and 406 ± 61 μm with the introduction of PLLA and PDLA, respectively. This further illustrates the importance of formulation conditions in influencing product properties and the adaptability of the method.

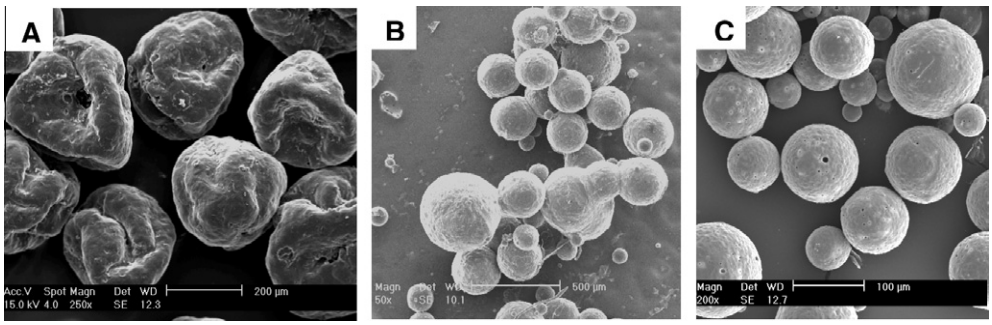

Fig. 6. SEM images of NIM_{slurry} produced using (A) PLGA alone, (B) PLGA/PDLA mix and (C) PLGA/PLLA. For the latter two mix, the PLA's were added to the [o] phase at a volume ratio of PLGA/PLA, 1/2 and all polymer were at the same concentration.

4. Conclusion

A protocol for producing a NIM system from a double emulsion has been described. During production of the NIMs, it is essential to ensure nanoparticle residency in the internal phase in order to maximise their entrapment. This method does not require expensive equipment and coupled with the fact that size and morphology can be readily adapted through alteration of formulation conditions, this makes it ideal for day-to-day drug delivery research.

Acknowledgements

This work carried out in the University of Birmingham, is part of a project investigating the production of particle-in-particle systems for chemoembolisation, funded by the Engineering and Physical Sciences Research Council (EPSRC), UK, Grant EP/G029059/1. The USP dissolution apparatus used in this research was obtained through Birmingham Science City: Innovative Uses for Advanced Materials in the Modern World (Advanced Materials 2), with support from Advantage West Midlands and part funded by the European Regional Development Fund. The assistance in cryo-SEM provided by Mrs. T. Morris from School of Metallurgy and Materials, and the confocal microscopy facility provided by Dr. S. Roberts from School of Cancer Studies, University of Birmingham are also acknowledged.

References

[1] O. Veiseh, J.W. Gunn, M. Zhang, Design and fabrication of magnetic nanoparticles for targeted drug delivery and imaging, Adv. Drug Delivery Rev. 61 (2010) 284–304.
[2] P. Pouponneau, J.C. Leroux, S. Martel, Magnetic nanoparticles encapsulated into biodegradable microparticles steered with an upgraded magnetic resonance imaging system for tumor chemoembolization, Biomaterials 30 (2009) 6327–6332.
[3] M. Jelvehgari, J. Barar, H. Valizadeh, N. Heidari, Preparation and evaluation of poly(ε-caprolactone) nanoparticles-in-microparticles by W/O/W emulsion method, Iranian J. Basic Med. Sci. 13 (2010) 85–96.
[4] J.O.H. Sham, Y. Zhang, W.H. Finlay, W.H. Roaa, R. Löbenberg, Formulation and characterization of spray-dried powders containing nanoparticles for aerosol delivery to the lung, Int. J. Pharm. 269 (2004) 457–467.
[5] K. Hadinoto, P. Phanapavudhikul, Z. Kewu, R.B.H. Tan, Dry powder aerosol delivery of large hollow nanoparticulate aggregates as prospective carriers of nanoparticulate drugs: effects of phospholipids, Int. J. Pharm. 333 (2007) 187–198.
[6] K. Ohashi, T. Kabasawa, T. Ozeki, H. Okada, One-step preparation of rifampicin/poly(lactic-co-glycolic acid) nanoparticle-containing mannitol microspheres using a four-fluid nozzle spray drier for inhalation therapy of tuberculosis, J. Control. Release 135 (2009) 19–24.
[7] F.Q. Li, C. Yan, J. Bi, W.L. Lv, R.R. Ji, X. Chen, J.C. Su, J.H. Hu, A novel spray-dried nanoparticles-in-microparticles system for formulating scopolamine hydrobromide into orally disintegrating tablets, Int. J. Nanomed. 2011 (2011) 897–904.
[8] M.D. Bhavsar, S.B. Tiwari, M.M. Amiji, Formulation optimization for the nanoparticles-in-microsphere hybrid oral delivery system using factorial design, J. Control. Release 110 (2006) 422–430.
[9] T. Mizoe, T. Ozeki, H. Okada, Preparation of drug nanoparticle-containing microparticles using a 4-fluid nozzle spray drier for oral, pulmonary, and injection dosage forms, J. Control. Release 122 (2007) 10–15.
[10] C. Gómez-Gaete, E. Fattal, L. Silva, M. Besnard, N. Tsapis, Dexamethasone acetate encapsulation into Trojan particles, J. Control. Release 128 (2008) 41–49.
[11] A.Z. Chen, Y. Li, F.T. Chau, T.Y. Lau, J.Y. Hua, Z. Zhao, D.K.W. Mok, Microencapsulation of puerarin nanoparticles by poly(L-lactide) in a supercritical CO_2 process, Acta Biomater. 5 (2009) 2913–2919.
[12] J. Kluge, F. Fusaroa, N. Casasa, M. Mazzotti, G. Muhrer, Production of PLGA micro- and nanocomposites by supercritical fluid extraction of emulsions: I. Encapsulation of lysozyme, J. Supercrit. Fluids 50 (2009) 327–335.
[13] K. Matsuyama, K. Mishima, Formation of TiO_2–polymer composite microparticles by rapid expansion of CO_2 saturated polymer suspensions with high shear mixing, J. Supercrit. Fluids 40 (2007) 117–124.
[14] P.J. Watts, M.C. Davies, C.D. Melia, Microencapsulation using emulsification/solvent evaporation: an overview of techniques and applications, Crit. Rev. Ther. Drug Carrier Syst. 7 (1990) 235–259.
[15] H. Takeuchi, H. Kojima, H. Yamamoto, Y. Kawashima, Evaluation of circulation profiles of liposomes coated with hydrophilic polymers having different molecular weights in rats, J. Control. Release 75 (2001) 83–91.
[16] R. Dinarvand, S.H. Moghadam, A. Sheikhi, F. Atyabi, Effect of surfactant HLB and different formulation variables on the properties of poly-D, L-lactide microspheres of naltrexone prepared by double emulsion technique, J. Microencapsul. 22 (2005) 139–151.
[17] J.C. Jeong, J. Lee, K. Cho, Effects of crystalline microstructure on drug release behavior of poly(ε-caprolactone) microspheres, J. Control. Release 92 (2003) 249–258.
[18] S.K. Sahoo, J. Panyam, S. Prabha, V. Labhasetwar, Residual polyvinyl alcohol associated with poly(D, L-lactide-co-glycolide) nanoparticles affects their physical properties and cellular uptake, J. Control. Release 82 (2002) 105–114.
[19] H. Murakami, M. Kobayashi, H. Takeuchi, Y. Kawashima, Preparation of poly(D, L-lactide-co-glycolide) nanoparticles by modified spontaneous emulsification solvent diffusion method, Int. J. Pharm. 187 (1999) 143–152.
[20] W. Abdelwahed, G. Degobert, H. Fessi, A pilot study of freeze drying of poly(ε-caprolactone) nanocapsules stabilized by poly(vinyl alcohol): formulation and process optimization, Int. J. Pharm. 309 (2006) 178–188.
[21] F. Boury, T. Ivanova, I. Panaïotov, J.E. Proust, A. Bois, J. Richou, Dynamic properties of poly(D, L-lactide) and polyvinyl alcohol monolayers at the air/water and dichloromethane/water interfaces, J. Colloid Interface Sci. 169 (1995) 380–392.
[22] M.F. Zambaux, F. Bonneaux, R. Gref, P. Maincent, E. Dellacherie, M.J. Alonso, P. Labrude, C. Vigneron, Influence of experimental parameters on the characteristics of poly(lactic acid) nanoparticles prepared by a double emulsion method, J. Control. Release 50 (1998) 31–40.
[23] D. Quintanar-Guerrero, A. Ganem-Quintanar, E. Allémann, H. Fessi, E. Doelker, Influence of the stabilizer coating layer on the purification and freeze-drying of poly(D, L-lactic acid) nanoparticles prepared by an emulsion–diffusion technique, J. Microencapsul. 15 (1998) 107–120.
[24] R.C. Mehta, R. Jeyanthi, S. Calis, B.C. Thanoo, K.W. Burton, P.P. Deluca, Biodegradable microspheres as depot system for parenteral delivery of peptide drugs, J. Control. Release 29 (1994) 375–384.